



## Ab initio study of the trapping of polonium on noble metals



Kim Rijpstra <sup>a,1</sup>, Andy Van Yperen-De Deyne <sup>a</sup>, Emilio Andrea Maugeri <sup>b</sup>,  
 Jörg Neuhausen <sup>b</sup>, Michel Waroquier <sup>a</sup>, Veronique Van Speybroeck <sup>a</sup>,  
 Stefaan Cottenier <sup>a,c,\*</sup>

<sup>a</sup> Center for Molecular Modeling (CMM), Ghent University, Technologiepark 903, 9052 Ghent, Belgium

<sup>b</sup> Laboratory for Radiochemistry, Paul Scherrer Institute (PSI), 5232 Villigen, Switzerland

<sup>c</sup> Department of Materials Science and Engineering, Ghent University, Technologiepark 903, 9052 Ghent, Belgium

### ARTICLE INFO

#### Article history:

Received 29 September 2015

Accepted 26 January 2016

Available online 29 January 2016

#### Keywords:

MYRRHA

LBE

Polonium

Adsorption

Ab-initio

### ABSTRACT

In the future MYRRHA reactor, lead bismuth eutectic (LBE) will be used both as coolant and as spallation target. Due to the high neutron flux a small fraction of the bismuth will transmute to radiotoxic <sup>210</sup>Po. Part of this radiotoxic element will evaporate into the gas above the coolant. Extracting it from the gas phase is necessary to ensure a safe handling of the reactor. An issue in the development of suitable filters is the lack of accurate knowledge on the chemical interaction between a candidate filter material and either elemental polonium or polonium containing molecules. Experimental work on this topic is complicated by the high radiotoxicity of polonium. Therefore, we present in this paper a first-principles study on the adsorption of polonium on noble metals as filter materials. The adsorption of monoatomic Po is considered on the candidate filter materials palladium, platinum, silver and gold. The case of the gold filter is looked upon in more detail by examining how bismuth pollution affects its capability to capture polonium and by studying the adsorption of the heavy diatomic molecules Po<sub>2</sub>, PoBi and PoPb on this gold filter.

© 2016 Elsevier B.V. All rights reserved.

The 4th generation of nuclear fission reactors will have to be inherently safer and more fuel-efficient than the nuclear power plants of today. The MYRRHA reactor, under development at SCK-CEN, will test the feasibility of 2 concepts: an accelerator driven system (ADS), and a lead bismuth cooled fast reactor [1,2]. In ADS mode, the chain of nuclear reactions can only be sustained if the combination of a proton accelerator and a spallation target feeds enough neutrons to the sub-critical core. The use of a liquid lead bismuth eutectic (LBE) both as coolant and as spallation target, will induce neutrons over a wide range of energies with little moderation, making MYRRHA a *fast* reactor. This will allow to transform the more abundant <sup>238</sup>U (abundance 99.3%) into <sup>239</sup>Pu which can be burned, rather than using only a limited fraction of natural uranium directly, i.e. <sup>235</sup>U (0.7%), as done in most present nuclear power reactors [3].

An issue with this type of reactors is the production of polonium as result of the transmutation of mainly bismuth. During the operation of MYRRHA, a non-negligible amount of polonium will be present in the LBE coolant. Part of the polonium will evaporate to the cover gas above the liquid LBE. Polonium has no stable isotopes. Its longest-lived isotopes, <sup>210</sup>Po (138.3 days), <sup>208</sup>Po (2.90 years) and <sup>209</sup>Po (102 years) are all strong  $\alpha$ -emitters. Because of the relatively short half-lives, polonium isotopes are strongly radioactive, e.g. 1 mg <sup>210</sup>Po has an activity of 166.25 GBq, while 1 mg of <sup>208</sup>Po reaches 21.74 GBq. As a result, polonium is highly radiotoxic upon inhalation. This makes it cumbersome to study, for instance, the thermodynamic properties of macroscopic quantities of polonium-containing molecules and solids experimentally [4,5].

In order to prevent a build-up of polonium and other malicious elements in the gas phase, the atmosphere inside MYRRHA's closed reactor vessel will be continuously filtered [1,6,7]. Developing appropriate filter systems requires an adequate knowledge of polonium chemistry. Exactly this is the bottleneck: due to the aforementioned difficulties the experimental information that is available in the literature is insufficient. Even worse: as most experimental studies date back to the 60's of the past century and

\* Corresponding author. Center for Molecular Modeling (CMM) and Department of Materials Science and Engineering, Technologiepark 903, BE-9052 Ghent, Belgium.

E-mail address: [stefaan.cottenier@ugent.be](mailto:stefaan.cottenier@ugent.be) (S. Cottenier).

<sup>1</sup> Now at SCK-CEN, Boeretang 200, 2400 Mol, Belgium.

earlier [8,9,5], merely reproducing them today is not easy with modern safety restrictions. In recent years, within the framework of ADS systems, much effort has been put into a better understanding of polonium and its interaction with LBE and different atmospheres: evaporation [10–13] or extraction [14,15] from LBE and the volatility of polonium molecules [16,4]. Also the use of transition metals and noble metals as filter materials is a subject of study [17]. Around 1980 a few studies on the adsorption and desorption of polonium from the gas phase on noble metals were performed by Gäggeler et al. [18,19].

Polonium, being experimentally hard to access, is an ideal example of a research topic where modern first principles methods can play a role. Available computational studies on polonium focus on its peculiar simple cubic ground state structure [20–22], on its role in the homologous series connecting selenium and tellurium with livermorium [23,24], or on it being a constituent of hypothetical semiconductors [25]. In all these cases, the relevance lies in a more fundamental understanding, rather than in practically useful polonium chemistry. A first computational effort into the latter direction has been delivered by Ayala et al. [26] in 2008 by studying the hydration of Po(IV) in solution. Rijpstra et al. [27] focusses on the interaction between polonium and LBE in the solid state. More recently the formation of several polonium-containing molecules, whose existence is expected in a LBE environment, has been studied in Van Yperen-De Deyne et al. [28]. In the present work we use density functional theory (DFT) to examine the interaction between a low concentration of monoatomic polonium and the surfaces of the candidate filter materials palladium, silver, platinum and gold. For the case of a gold filter, we investigate the adsorption of the diatomic molecules Po<sub>2</sub>, PoPb and PoBi and the effect of bismuth pollution.

## 1. Methods

### 1.1. Computational settings

All calculations in this work are performed within density functional theory (DFT) [29,30] as implemented in the ‘Vienna ab initio simulation package’ (VASP) [31]. The projector augmented wave (PAW) method [32,33] is used to solve the scalar-relativistic Kohn–Sham equations. The exchange–correlation energy is described by the Perdew–Burke–Ernzerhof (PBE) functional [34]. VASP incorporates by default scalar relativistic effects [35]. Since we are dealing with mainly heavy elements, the next order of relativistic effects, spin–orbit coupling (SO), is taken into account self-consistently [36,37].

VASP is a periodic code in which all observable properties of a crystal can be expressed as integrals over the unit cell (first Brillouin zone) of the reciprocal space. Through the Bloch theorem [38], the wavefunction for every point in reciprocal space is represented by a Fourier series of plane waves. Two parameters determine most of the computational precision. One of these is the *k*-point grid that is used to sample the integral over the first Brillouin zone. The second parameter is the energy of the last plane wave in the Fourier series, the so-called cut-off energy. In order to find a good balance between computational precision and computational cost, we computed for face centred cubic (fcc) gold and fcc palladium the energy difference between the ground state volume and a 5% expanded volume, for a wide range of both *k*-grid densities and cut-off energies. We concluded that  $\Gamma$ -centred Monkhorst–Pack *k*-grids [39] with a density of 216000 *k*-points/Å<sup>−3</sup> and a cut-off energy of 330 eV were sufficient to obtain a numerical accuracy for energy differences better than 0.001 eV/atom for gold and 0.002 eV/atom for palladium. For the molecular adsorption calculations a cut-off energy of 550 eV was used, leading to even

smaller errors. Fermi level smearing of 0.01 eV (bulk calculations) or 0.1 eV (surface calculations) was used with the first order Methfessel–Paxton method [40]. During geometry optimization, we considered a structure converged when all forces on the atoms are below 0.01 eV/Å, unless the atoms were kept fixed within the cell.

One of the quantities required to determine the adsorption enthalpy is the energy  $E_u$  of the free adsorbent *u* (see Eq. (1) later on in Section 1.3.1). Preferentially, these calculations should be performed within the same periodic code as applied for the slab on which *u* will be adsorbed. Sufficiently large unit cell sizes should be taken into consideration to avoid interaction with periodic images of *u*. While we use cells of 15 Å × 15 Å × 15 Å for the monoatomic energies, for the diatomic molecules we consider unit cells of dimension 15 Å × 15 Å × 18 Å, with the largest size in the direction of the internuclear axis of the molecule. The energies obtained for molecules in these large empty unit cells should be comparable with non-periodic calculations, obtained in a non-periodic code using the same DFT functional.

### 1.2. Level of theory

In order to assess the level of theory that will be required, we compare in Fig. 1 formation enthalpies for Po<sub>2</sub>, PoPb and PoBi (the formation enthalpy  $\Delta H_{form}$  is the difference between the free molecule enthalpy  $E_u$  and the sum of the free atom enthalpies). These formation enthalpies are computed by three different methods: at one hand a high level method – Multi-Reference Configuration Interaction (MRCI) by the non-periodic ORCA code, and at the other hand either the regular PBE functional or the more expensive hybrid PBE0 functional, both by the periodic VASP code. The influence of inclusion of exact Fock exchange is examined by comparing a pure functional (PBE) and a hybrid functional (PBE0).

In Ref. [28], it was already shown that PBE0 succeeds surprisingly well in reproducing the formation energies obtained by the much more accurate MRCI method, within 0.2 eV. From Fig. 1a and b, it can be seen that the PBE functional follows the PBE0 results closely. When calculating a linear regression for all PBE values obtained with VASP against those obtained for PBE0, both with and without SO and including the hypothetical solid PoAu as an additional case, we find  $\Delta H_{form}(PBE) = 1.09 \Delta H_{form}(PBE0) - 0.17$  eV/*u* with a standard error on the PBE values of 0.10 eV/*u*. Considering these small differences, and considering the fact that adsorption calculations are intrinsically much more time-consuming than free molecule calculations, we conclude that it is justified to perform the adsorption calculations with the less expensive PBE functional.

Whereas MRCI and PBE/PBE0 are in fair agreement with each other when no spin–orbit interaction is included (Fig. 1a), this agreement vanishes upon adding spin–orbit coupling (Fig. 1b). In the latter case, there is very little spread in the DFT results, while for MRCI a much larger difference between the three molecules is found. This can be understood when considering the interplay of symmetry and degeneracy: a diatomic molecule has a high symmetry, which leads to degeneracy of several molecular orbitals. When such degeneracies are present, a high-level multireference method as MRCI leads to results that are different from what is obtained by regular single-reference DFT, with the former being the more accurate one. In the absence of degeneracies – as happens for low-symmetry cases – both methodologies lead to much more similar results. The case of a molecule on a surface has a reduced symmetry, and therefore the deviation by PBE/PBE0 is expected to be much smaller for adsorption energies. Another feature that contributes to the deviation in Fig. 1b is the fact that spin–orbit coupling is treated in different ways in both codes: perturbatively in ORCA (MRCI) and self-consistently in VASP (PBE/PBE0). The latter is more correct. Concerning the differences between the GGA (PBE)

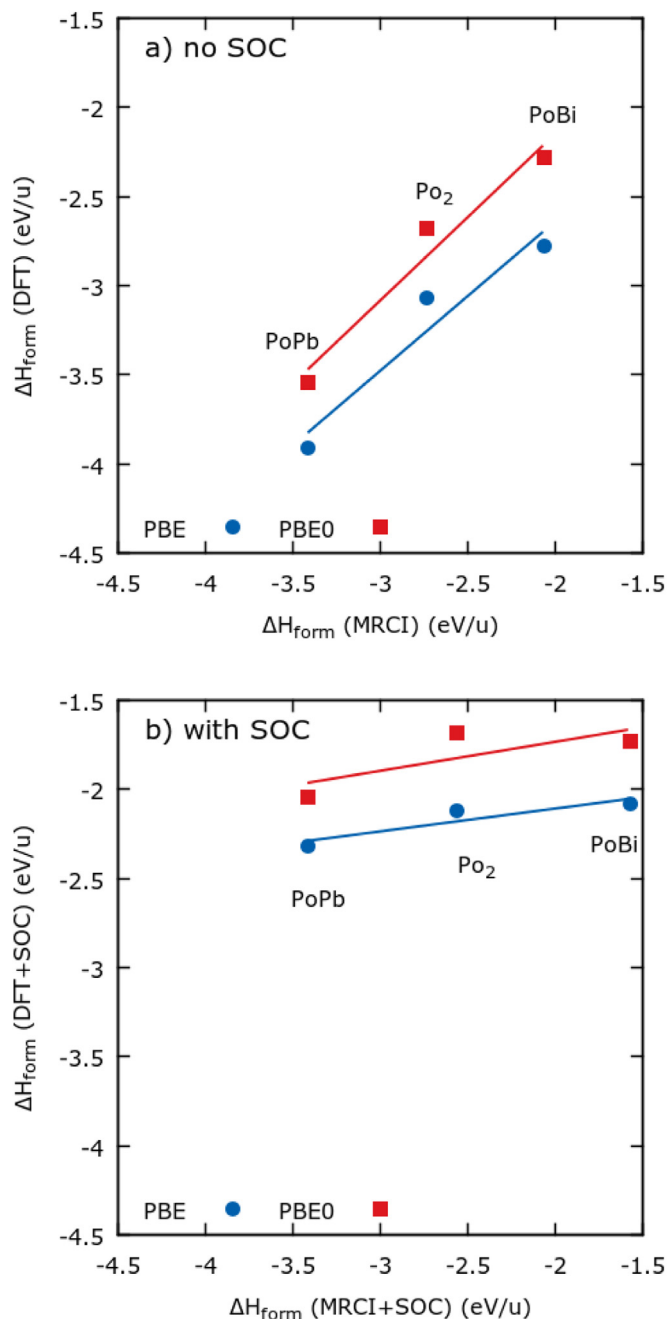


**Fig. 1.** The DFT formation enthalpies versus those obtained with MRCI: a) without SO, b) with SO.

and hybrid (PBE0) density functional, Fig. 1 clearly shows that both represent a qualitatively very similar picture.

Based on these considerations and the high computational cost of simulations with both hybrid functionals and spin–orbit interactions, we chose to apply periodic DFT with the PBE functional including spin–orbit coupling to determine the adsorption energies in this work. This choice is corroborated by successful examples found in literature. In Refs. [41,42] similar methods were used for the calculation of cohesion energies and found good agreement with experiment. These data are compared in Ref. [43] to a higher-level method, and were found to be acceptable. A similar story holds for Ref. [44], where adsorption energies for platinum clusters on graphene were obtained with similar methods

as in our work.

### 1.3. Surface slabs & adsorption enthalpies

For a computational study of adsorption we need a reliable model for the surface where the adsorbate can adsorb on. In a periodic code the surface slab is modelled to be infinite in two dimensions. The third dimension shows a number of atomic layers of adsorbent, terminated with a sufficiently large vacuum to prevent interaction between the adjacent periodic images in that dimension. In order to prevent polarization of the vacuum, due to the charge build-up in the adsorbates, the slabs are made symmetrical: adsorption will take place on both the top and the down side, see Fig. 2d.

In order to significantly reduce the repulsive effects between the adsorbates, the number of layers should be sufficiently large. However, adsorption calculations with such large cells are computationally very expensive. In this work, the number of layers in the slab is limited to seven, which is sufficient to obtain correct interlayer distances near the surface in complete consistency with what has been proposed in Ref. [45]. In the geometry optimization of the slab, the positions of the atoms lying in the central layer are kept fixed at the equilibrium bulk values. Also the lattice vectors were frozen to mimic the presence of a bulk material in the middle of the slab. In the fixed cell all other layers are free to relax as well as the adsorbed atom(s). This model gives a good balance between computational cost and accuracy. An assessment study learns that slabs with 5 and 9 layers deviate less than 0.02 eV/Po for the adsorption enthalpy of monoatomic polonium. It proves that the choice of 7 layers is an acceptable estimate. Another specific parameter for an accurate prediction of adsorption enthalpies in periodic calculations is the size of the vacuum taken into consideration in the unit cell. It has to be large enough to prevent interaction between the adsorbates on top of one slab and the periodic image of the adsorbate at the adjunct side (see Fig. 2d). After evaluating the adsorption of polonium on a Au(100) surface for

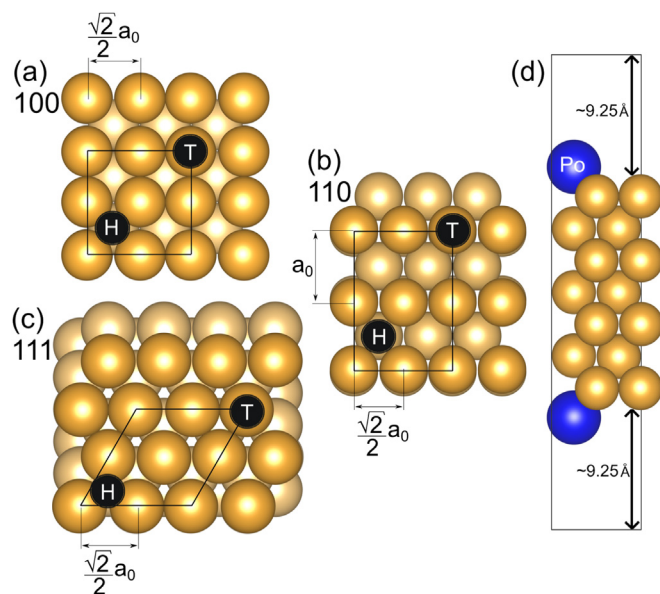


**Fig. 2.** a, b, c: surface topographies for Au(100), Au(110) and Au(111). The hollow and the top site are indicated. The darker colour marks the top layers. The lines show the size of the used  $2 \times 2$  primitive unit cells. d: the side view of polonium adsorption on a hollow site of Au(100) as is calculated in this work. The total size of the vacuum is the sum of both vacua. (For interpretation of the references to colour in this figure legend, the reader is referred to the web version of this article.)

several vacuum sizes, a width of 18.5 Å turns out to be reassuringly sufficient.

### 1.3.1. Adsorption and surface periodicity

The adsorption enthalpy of a single atom or molecule  $u$ , hereafter called unit, on an infinitely (*inf*) large surface is defined as:

$$\Delta H_{ads}^{inf}(u) = \frac{E_{slab+u}^{inf} - E_{slab}^{inf} - N_u E_u}{N_u} \quad (1)$$

$\Delta H_{ads}$  is the adsorption enthalpy per adsorbed unit expressed in eV/u,  $E_u$  represents the energy of the free unit, while  $N_u$  denotes the number of adsorbed units, which is even due to the symmetric nature of the model slab. The superscript (*inf*) refers to a single adsorbed unit on a infinite surface. This picture cannot be generated in a periodic calculation, as the periodic cell is finite and the adsorbed unit can interact with its periodic images. In order to represent the ideal single adsorption case, the distance between these periodic images should be sufficiently large to prevent any spurious interaction between them. This would lead to highly expensive calculations. It is therefore necessary to use smaller surface unit cells and to correct for the spurious effects. In Fig. 3, a correction scheme is suggested for the adsorption enthalpy in a finite periodic unit cell (*fin*). Periodic codes yield an adsorption enthalpy  $\Delta H_{ads}^{fin}(u)$  for a single unit  $u$  on a surface that is composed of periodic images of a finite slab with an adsorbed unit  $u$ . The correction term  $Q_{fin}$  should be subtracted from  $\Delta H_{ads}^{fin}(u)$  to approach  $\Delta H_{ads}^{inf}(u)$ . This term is estimated by the interaction between the adsorbed unit  $u$  and its periodic images in absence of the surface, which captures most of the spurious interaction. Summarizing, a computable expression for the infinite adsorption enthalpy is given by:

$$\Delta H_{ads}^{inf}(u) \approx \Delta H_{ads}^{fin}(u) - Q_{fin} \quad (2)$$

$$\approx \frac{E_{slab+u}^{fin} - E_{slab}^{inf} - N_u (E_u + Q_{fin})}{N_u}$$

We note that the energy per slab atom in the absence of unit  $u$  is obviously independent of the dimension of the slab:  $E_{slab}^{inf} = E_{slab}^{fin}$ . Eq. (2), graphically depicted in Fig. 3, is valid both for atoms and molecules. Molecules undergo a deformation upon adsorption, which is taken into account in the determination of  $Q_{fin}$  by considering the cell for the adsorbed case with all slab atoms removed and the molecule kept in its deformed state. For an atom, it suffices to perform a calculation within the same finite surface unit cells, as used for the evaluation of  $E_{slab+u}^{fin}$ , dropping all slab

atoms and keeping only the single atom  $u$  in the empty slab cell.

### 1.3.2. Adsorption of monoatomic polonium

For the adsorption of monoatomic polonium and bismuth, we chose to make  $2 \times 2$  primitive cells, so that each layer has 4 atoms, see Fig. 2. Adsorbing one polonium atom on both surfaces of the cell is equivalent to the deposition of a quarter monolayer, ensuring a separation of at least 5.6 Å between periodic images. This is sufficiently large to simulate the adsorption of an isolated atom [46,47]. For the  $2 \times 2$  slabs, grids of  $8 \times 8 \times 1$  k-points are used, equivalent to the aforementioned setting. Only one k-point needs to be taken in the z-direction due to the considerable length of the cell and the negligible interaction between the images in this direction. The periodic correction  $Q_{fin}$  in these cells, compared to a single polonium atom in a box of 15 Å, varies between 0.000 eV/Po for the Bi(100), and  $-0.056$  eV/Po, for the (100) and (110) palladium- and platinum surfaces, depending on the size of the surface unit cell. By comparing the adsorption energies for the case of monoatomic polonium on Au(100) obtained with the settings described in Section 1.1 and with more stringent settings, we conclude that the numerical uncertainty on the adsorption energy is about 0.003 eV/Po.

All four noble metals (palladium, platinum, silver and gold) have a fcc crystal structure as ground state. In order to get a good picture of the adsorption behaviour on these noble metals, three low-index surfaces were constructed: (111), (100), (110), see Fig. 2. The (111) surface is the most closed-packed one, (110) has the most rough topography with trenches and lines, (100) falls in between these two extremes. For completeness, the surface energies  $H_{surf}$  (eV/Å<sup>2</sup>) are included in Table 1 and they are defined as:

$$\Delta H_{surf} = \frac{E_{slab} - N_{slab} E_{bulk}}{2 A_{slab}} \quad (3)$$

with  $N_{slab}$  the number of atoms in the slab,  $A_{slab}$  its surface area and  $E_{bulk}$  the energy per atom of the original bulk material. As expected, the more open surfaces have larger surface energies, a consequence of the higher number of atoms with a lower coordination compared to the bulk [48]. Surface energies reported in literature [48,45] can be up to 75% higher than those found in this work. A large part of this discrepancy is attributed to the choice of the PBE functional, as confirmed by Da Silva et al. [45].

### 1.3.3. Adsorption of molecules

To study the adsorption of Po<sub>2</sub>, PoBi and PoPb, the Au(100)-surface was chosen. The  $2 \times 2$  or  $2 \times 1$  primitive surface cell however, is too small to allow a wide variety of adsorption scenarios. Therefore the cell is enlarged to a  $3 \times 2$  surface (k-grid of  $6 \times 8 \times 1$  k-points). Hence different starting orientations for each diatomic molecule can be studied without direct contact between the periodic images. The spurious effects due to periodicity ranged from 0.038 to  $-0.389$  eV/u for the different adsorptions.

## 2. Results and discussion

### 2.1. Polonium on clean noble metals

In Table 1, we evaluate the adsorption behaviour of single polonium atoms on the 4 noble metals, systematically for the (100) (110) and the (111) surfaces. For each of these surface orientations, one could consider three plausible adsorption positions: top, bridge and hollow site. For the test case of Ag(111), it was observed that the polonium atom shifted from the bridge position to a hollow site. In a second attempt, with the in-plane position of polonium fixed on the bridge site, a value for the adsorption enthalpy of 0.06 eV/Po

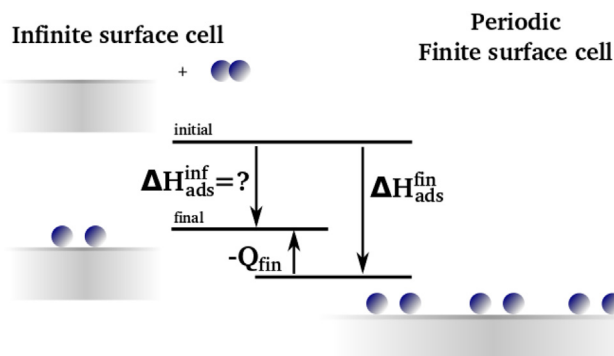


Fig. 3. Scheme for the calculation of adsorption enthalpies using a periodic code.  $Q_{ads}$  correction due to the self-interaction between periodic images of adsorbed molecules.

**Table 1**

Surface energies and adsorption enthalpies for polonium and bismuth on slabs composed of different noble metals and different orientations of the surface. The surface orientations are ordered from closed to open topologies.

	Surface (eV/Å <sup>2</sup> )			Top site (eV/Po)			Hollow site (eV/Po)			Hollow site (eV/Bi)		
	(111)	(100)	(110)	(111)	(100)	(110)	(111)	(100)	(110)	(111)	(100)	(110)
Pd	0.083	0.095	0.100	-2.30	-2.32	-2.08	-3.10	-3.74	-3.83	-3.51	-4.06	-4.21
Pt	0.089	0.113	0.114	-2.07	-2.19	-2.19	-3.01	-3.86	-3.64	-3.61	-4.36	-4.22
Ag	0.045	0.050	0.054	-1.64	-1.53	-1.41	-2.11	-2.43	-2.54	-2.08	-2.40	-2.58
Au	0.047	0.056	0.058	-1.44	-1.44	-1.49	-2.09	-2.52	-2.54	-2.35	-2.89	-2.92

above the value for the hollow site was found, still well under the value for the top site. As the adsorption behaviour on the three surface orientations for all four noble metals shows high similarity (see Table 1), bridge positions were no longer considered as possible stable adsorption sites for the other noble metals and surfaces. Bridge positions form the transition states between two hollow sites. Due to the size of the polonium atom and its effect on the upper layers, also intermediate positions, such as the pseudo-threefold on (110) [49], are not considered. For every surface, Po adsorption on the top and hollow sites are calculated (see Fig. 2). For the (111)-orientation, the ‘fcc’ position is chosen: a hollow site with no atom underneath in the second layer.

As can be seen in Table 1 Po is predicted to spontaneously adsorb on all noble metals, with adsorption enthalpies varying from -2.1 to -3.9 eV. For all four adsorbents we observe the same behaviour: the hollow site is preferred over the top site by 0.4–1.8 eV. The more open topographies (100) and (110) show stronger adsorption (up to 0.7 eV) on the hollow sites than the close-packed (111) surface. This is in contrast with the adsorption on top sites. The difference in adsorption enthalpies here is much smaller for different surface orientations, ranging from 0.0 to 0.3 eV. No general trend concerning the topography can be deduced here. The influence of the more open surfaces is not surprising due to the higher surface energies: there is more energy to gain from adsorption.

Even though all four noble metals show similar behaviour, there are significant quantitative differences, with gold and silver on one side and palladium and platinum on the other. The adsorption enthalpies for the group 10 noble metals are between 0.6 and 1.3 eV more negative than for gold and silver of group 11. Within the groups themselves the enthalpies only vary up to 0.3 eV at most, often less. These values agree reasonably well with the experimental adsorption enthalpies obtained by Gäggeler et al. [18,19]: gold (2.00–2.34 eV/Po) and palladium (3.01–3.38 eV/Po), somewhat less for platinum (1.94–2.90 eV/Po) and for silver (1.71 eV/Po). For platinum there is a wide spread in the experimental results, which is probably due to reproducibility issues and for silver only one measurement is found.

## 2.2. Bismuth on clean noble metals

Because polonium is not the only element present in the cover gas above the LBE, it is relevant to study the adsorption behaviour on noble metals for other elements in the gas phase. Bismuth is known to have a relatively high vapour pressure above liquid LBE [50,51]. The number of bismuth atoms in the reactor atmosphere will be many orders of magnitude higher than the number of polonium atoms. To get an idea of the behaviour of elemental bismuth near noble metals we repeated the calculations on all surfaces for the hollow sites only, replacing polonium with bismuth, see Table 1.

For all noble metals except silver, larger adsorption enthalpies are found. Silver has no preference towards Bi or Po adsorption. For

gold and palladium, adsorbing bismuth instead of Po leads to an extra energy reduction between 0.2 and 0.4 eV. For platinum this goes up to 0.5 and even 0.6 eV per adsorbed atom. It is therefore clear that elemental bismuth will show strong adsorption behaviour near noble metal surfaces and that it might saturate the filter, preventing further Po capture.

## 2.3. Polonium on polluted gold

Will a bismuth-polluted filter surface still be able to capture Po, and if so, how strongly? Several scenarios were taken into consideration to answer these questions. The starting point was always the 7 layers Au(100) slab, on which each time a different pollution layer was built: a 50%–50% gold-bismuth layer (50% of the surface gold atoms are replaced by bismuth, Fig. 4a), a 50% and a 75% bismuth layer (respectively 2 and 3 out of 4 hollow sites on the gold surface occupied by bismuth, Fig. 4b and c). A fourth scenario is the adsorption of Po on a pure bismuth slab (Fig. 4d). This slab is constructed from the rhombohedral phase of bismuth described in a hexagonal unit cell (hcp), in the same manner as the noble metal slabs.

For the slabs covered by 50% and 75%, the adsorption of this rather large amount of bismuth atoms turns out to be energetically favourable still, with enthalpies of -2.63 and -2.34 eV/Bi. The Bi(001) slab has a surface energy of 0.029 eV/Å<sup>2</sup>, which is significantly lower than for noble metal surfaces. The 50%–50% gold bismuth layer, is a hypothetical surface that will never spontaneously form, because it has bismuth cramped into small spaces, originally occupied by a gold atom. Nevertheless, this can serve as a model for a mixed Au–Bi environment.

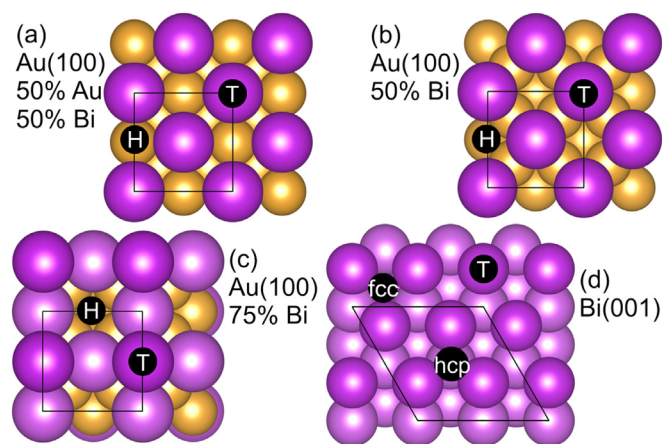


**Fig. 4.** a, b, c: the three with bismuth polluted gold slabs. At figure the top and hollow site are indicated. d: the Bi(100) with top and deep hollow site indicated. In (a) the Au and Bi atoms are in the same surface in contrast to (b) and (c) in which the top layer only contains Bi and not fully occupied. The darker colour in (d) serves to mark the top layer. (For interpretation of the references to colour in this figure legend, the reader is referred to the web version of this article.)

In Table 2 the adsorption enthalpies for polonium on these layers are given for both hollow and top sites. Herein the combined system of gold and bismuth is seen as ‘the slab’. Each of the slabs again has 7 layers, even though the outermost layers are broadened to fit in the bismuth atoms, see Fig. 4. The bridge position is only calculated in the case of 75% bismuth and resulted into an adsorption enthalpy of  $-1.49$  eV/Po, a value that is intermediate between those for the top and hollow site. For the 50%–50% slab, the hollow site is the position on top of the open gold atom: equivalent to a top-site on a clean gold surface, but surrounded by 4 bismuth atoms. On the pure bismuth slab there are two distinct hollow sites: one with a bismuth atom on the second layer beneath the hollow site, known as the hcp site, and one without, the fcc site. For polonium, this fcc site is preferred, having an adsorption enthalpy that is  $0.14$  eV/Po more negative than for the other site.

Again, the hollow site is preferred in all cases. On bismuth a decent  $-1.84$  eV/Po is found. The fcc site is preferred here, because it allows polonium to sink somewhat deeper into the first layer, bringing it closer to 3 bismuth atoms on the second layer, instead of only one (for the hcp site). The 50%–50% slab could be considered as a surface on which some bismuth is present, but the polonium can still reach the gold. The hollow site here delivers an adsorption enthalpy of  $-1.90$  eV/Po, which is weaker than adsorption on a hollow site on pure gold, but better than adsorption on a top position there. The higher coordination of polonium thanks to the nearby bismuth, thus has a positive effect on the adsorption. The worst adsorption behaviour is found on the 50% bismuth surface, both on top and hollow site. The main difference with the 50%–50% slab is that polonium is not able to bind to the gold directly. For the 75% slab the enthalpies are in between those for the 50% and the pure bismuth.

The adsorption behaviour of polonium on these slabs is determined by its coordination possibilities and the vicinity of gold, which is preferred over bismuth as a bonding partner of polonium. Due to the strong interaction between bismuth and gold, the adsorption of polonium deteriorates on bismuth atoms directly in contact with the gold slab. Summarising, even weakened by bismuth-pollution, adsorption of elemental polonium on gold filters remains a strong exothermic process.

#### 2.4. Adsorption of polonium molecules

We know from Section 2.1 and 2.2, that for polonium and bismuth adsorption the hollow site is strongly preferred on noble metals. It therefore seems highly unlikely that any of the heavy diatomic molecules ( $\text{Po}_2$ ,  $\text{PoPb}$ ,  $\text{PoBi}$ ) can adsorb on gold without occupying at least one hollow site. One can imagine three possible adsorption scenarios for which the bond length of the free molecule is initially conserved, see Fig. 5a–c: atom B on top of adsorbed atom A, A and B adsorbed in two neighbouring hollow sites (bonding over the bridge site) and B on top of a gold atom bound to adsorbed A located in a hollow site. The first scenario is similar to the situation which was already been studied for polonium on

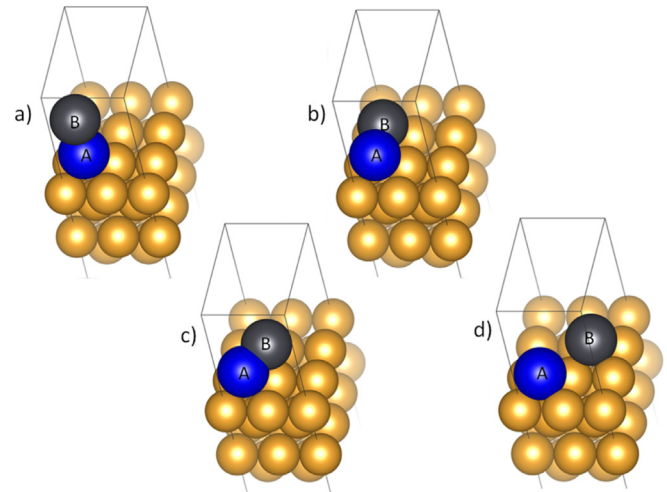


Fig. 5. Different adsorption scenarios for diatomic heavy molecules. a, b and c are initial states, the fourth scenario d is a possible result for relaxation from c.

bismuth (Section 2.3) and will now only be repeated for bismuth and lead on top of polonium. In all of these cases it was clear that adsorption with perpendicular orientation to the surface is far from stable. The top-scenarios (Fig. 5a) in this work have enthalpies more than  $1.80$  eV/u above the optimum. The situation with atom A in a hollow site and B on top of a gold atom (Fig. 5c) evolved upon relaxation in some cases to a fourth situation (Fig. 5d): A and B in diagonally connected hollow sites, which effectively means the molecule has been broken. This happened for the cases where the bismuth and lead atoms were placed on top of a gold atom, while the polonium atom was placed in a hollow site from the start. For polonium as atom B with bismuth or lead as atom A in a hollow site (Fig. 5c), the molecule stayed together by pushing atom A slightly out of the optimal hollow site. The bonding distance for these scenarios increased to  $\approx 3.0$  Å and the adsorption enthalpy is more than  $0.8$  eV/u above optimum (Fig. 5b for  $\text{PoBi}$  and  $\text{PoPb}$ ; Fig. 5d for  $\text{Po}_2$ ). Based on these results, other starting orientations, the top scenarios,  $\text{Po}$  on  $\text{Po}$  and  $\text{Po}$  on  $\text{Pb}$  and the adsorption of  $\text{Po}_2$  on one top and one hollow site were not considered.

Looking at Table 3, it is clear that all three diatomic molecules have a strong tendency towards adsorption on gold. Of all considered polonium molecules,  $\text{Po}_2$  will be the most volatile. While  $\text{PoBi}$  and  $\text{PoPb}$  tend to stick together in 2 neighbouring hollow sites,  $\text{Po}_2$  will tend to break up into separate atoms. This is not only clear from the adsorption enthalpies, but can also be seen by comparing the distance between the two adsorbed atoms in neighbouring hollow sites: for  $\text{PoBi}$  and  $\text{PoPb}$  the distance is about 121% of the original bonding distance, for  $\text{Po}_2$  this is about 128%. These distances increase by more than  $0.5$  Å, compared to an original  $2.7$ – $2.8$  Å, when

Table 2  
Adsorption enthalpies for Po on Bi polluted Au(100). The different scenarios are shown in Fig. 4.

	Surface	(100) (eV/Po)	
		Hollow	Top
Au	50% Bi 50% Au	-1.90	-1.13
Au	50% Bi	-1.60	-0.95
Au	75% Bi	-1.65	-1.33
Bi	100% Bi	-1.84	-1.27

Table 3  
Adsorption enthalpies for  $\text{Po}$ ,  $\text{Po}_2$ ,  $\text{PoBi}$  and  $\text{PoPb}$  into two hollow sites on gold, given in eV/u wherein u stands for one unit of the specified molecule. Also the distance between both ions is given each time. The bold values represent the lowest energy scenarios.

	Neighbour			Separated	
	$R_{mol}$ (Å)	$R_{ads}$ (Å)	$H_{ads}$ (eV/u)	$R_{ads}$ (Å)	$H_{ads}$ (eV/u)
Po	/	/	-2.62	/	/
$\text{Po}_2$	2.81	3.59	-2.41	<b>4.48</b>	<b>-2.45</b>
$\text{PoBi}$	2.76	<b>3.35</b>	<b>-2.98</b>	4.41	-2.77
$\text{PoPb}$	2.73	<b>3.30</b>	<b>-2.73</b>	4.31	-2.28

both atoms are adsorbed in two neighbouring sites. This analysis also shows that for all the molecules, the dissociated structure is highly preferred and a situation with atoms located at one hollow and one top site are only metastable structures. It is interesting to see that both PoBi and PoPb yield larger adsorption enthalpies than monoatomic polonium, while Po<sub>2</sub> does not.

### 3. Conclusions

In this work we studied the adsorption behaviour of polonium on the noble metals silver, gold, palladium and platinum, using a first principles method. Strong adsorption behaviour of elemental polonium was found for all noble metal surfaces, with a maximum of  $-3.6$ – $-3.8$  eV/Po for palladium and platinum, compared to  $-2.5$  eV/Po for gold and silver. The values computed for the (111)-surfaces nicely agree with experimental elemental polonium adsorption energies that were reported by Gaggeler et al. [18,19]. It was found that polonium always prefers sites that lead to a higher coordination. Also, the adsorption behaviour of polonium on bismuth polluted gold slabs has been studied, as well as on bismuth itself. For the latter, the strongest adsorption was 0.7 eV/Po weaker than for gold. For all other cases coordination played an important role, as well as the binding partners of polonium: as long as contact with the gold surface can be maintained, the adsorption enthalpies will approximate those for pure gold. When polonium can only bind to bismuth atoms, nearby gold will actually weaken the Bi–Po bonding. The heavy diatomic polonium molecule will split upon adsorption on noble metals. PoBi and PoPb are less volatile in contact with gold than monoatomic polonium, having adsorption enthalpies of  $-3.0$ – $-2.7$  eV/molecule. Their two atoms will occupy two neighbouring hollow sites. The Po<sub>2</sub> molecule is slightly more volatile in contact with gold than monoatomic polonium.

In terms of filter design, the conclusions of this work are four-fold. (1) Among the four studied noble metals, palladium and platinum are the best filters to capture elemental polonium. (2) Bismuth contamination does deteriorate the filter performance, but does not render it useless. (3) The molecules PoBi or PoPb are more easily captured by a gold filter than elemental polonium. The majority of binary molecules dissociate and both atoms will occupy a hollow site on the filter surface, while a smaller part could occupy a metastable hollow-top configuration without full molecular dissociation. (4) If Po<sub>2</sub> is formed, which is highly unlikely due to the low concentrations in MYRHHA, it will be slightly more volatile.

### Acknowledgements

This work is supported by the European Commission through the FP7 project SEARCH (Safe ExploitAtion Related CHemistry for HLM reactors, Project Nr. 295736) and by the Research Board of Ghent University. The authors acknowledge helpful discussions with Alexander Aerts (SCK-CEN, Mol). Stefaan Cottenier acknowledges financial support from OCAS NV by an OCAS-endowed chair at Ghent University. Calculations were carried out using the Stevin Supercomputer Infrastructure at Ghent University, funded by Ghent University, the Hercules Foundation, and the Flemish Government (EWI Department).

### References

- [1] H.A. Abderrahim, P. Kupschus, E. Malambu, P. Benoit, K. Van Tichelen, B. Arien, F. Vermeersch, P. Dhondt, Y. Jongen, S. Ternier, et al., Myrrha: A multipurpose accelerator driven system for research & development, nuclear instruments and methods in physics research section A: accelerators, spectrometers, Detect. Assoc. Equip. 463 (3) (2001) 487–494.
- [2] J. Zhang, Lead-Bismuth Eutectic (LBE): a coolant candidate for Gen. IV advanced nuclear reactor concepts, Adv. Eng. Mater. 16 (4) (2014) 349–356.
- [3] H.A. Abderrahim, P. Baeten, D. De Bruyn, R. Fernandez, Myrrha—a multi-purpose fast spectrum research reactor, Energy Convers. Manag. 63 (2012) 4–10.
- [4] B. Eichler, Die Flüchtigkeitseigenschaften des Poloniums, Paul Scherrer Institute Annual Report 02–12, Villigen, Switzerland, 2002.
- [5] K. Bagnall, The chemistry of polonium, Q. Rev. Chem. Soc. 11 (1) (1957) 30–48.
- [6] T. Obara, Y. Yamazawa, T. Sasa, Polonium decontamination performance of stainless steel mesh filter for lead alloy-cooled reactors, Prog. Nucl. Energy 53 (7) (2011) 1056–1060.
- [7] E. Loewen, Investigation of polonium removal systems for lead-bismuth cooled fbrs, Prog. Nucl. Energy 47 (14) (2005) 586–595.
- [8] M. Whitaker, W. Bjorksted, A.C. Mitchell, Preliminary report on a quick method of depositing polonium on silver, Phys. Rev. 46 (7) (1934) 629.
- [9] P.E. Figgins, The Radiochemistry of Polonium, vol. 3037, National Academies, 1961.
- [10] J. Buongiorno, C. Larson, K. Czerwinski, Speciation of polonium released from molten lead bismuth, Radiochim. Acta 91 (3) (2003) 153–158.
- [11] B.G. Prieto, J. Van den Bosch, J. Martens, J. Neuhausen, A. Aerts, Equilibrium evaporation of trace polonium from liquid lead–bismuth eutectic at high temperature, J. Nucl. Mater. 450 (2014) 299–303.
- [12] S. Ohno, Y. Kurata, S. Miyahara, R. Katsura, S. Yoshida, Equilibrium evaporation behavior of polonium and its homologue tellurium in liquid lead–bismuth eutectic, J. Nucl. Sci. Technol. 43 (11) (2006) 1359–1369.
- [13] J. Neuhausen, B. Eichler, U. Köster, Investigation of evaporation characteristics of polonium and its lighter homologues selenium and tellurium from liquid Pb–Bi–eutecticum (CERN-PH-EP-2004-061), Radiochim. Acta 92 (2004) 917–923.
- [14] S. Heinitz, J. Neuhausen, D. Schumann, Alkaline extraction of polonium from liquid lead bismuth eutectic, J. Nucl. Mater. 414 (2) (2011) 221–225.
- [15] T. Obara, T. Miura, Y. Fujita, Y. Ando, H. Sekimoto, Preliminary study of the removal of polonium contamination by neutron-irradiated lead–bismuth eutectic, Ann. Nucl. Energy 30 (4) (2003) 497–502.
- [16] E.A. Maugeri, J. Neuhausen, R. Eichler, D. Piguet, T.M. Mendonça, T. Stora, D. Schumann, Thermochromatography study of volatile polonium species in various gas atmospheres, J. Nucl. Mater. 450 (1) (2014) 292–298.
- [17] J. Neuhausen, B. Eichler, Extension of Miedema's Macroscopic Atom Model to the Elements of Group 16 (O, S, Se, Te, Po), PSI-report 03–13, Paul Scherrer Institute, Villigen, Switzerland, September 2003.
- [18] B. Eichler, H. Gaggeler-Koch, H. Gaggeler, Thermochromatography of carrier-free elements: polonium in copper columns, Radiochim. Acta 26 (3–4) (1979) 193–196.
- [19] H. Gaggeler, H. Dornhöfer, W. Schmidt-Ott, N. Greulich, B. Eichler, Determination of adsorption enthalpies for polonium on surfaces of copper, silver, gold, palladium and platinum, Radiochim. Acta 38 (1985) 103–106.
- [20] D. Legut, M. Friák, M. Sob, Why is polonium simple cubic and so highly anisotropic? Phys. Rev. Lett. 99 (1) (2007), 016402–016402.
- [21] M.J. Verstraete, Phases of polonium via density functional theory, Phys. Rev. Lett. 104 (3) (2010) 035501.
- [22] C.-J. Kang, K. Kim, B. Min, Phonon softening and superconductivity triggered by spin-orbit coupling in simple-cubic  $\alpha$ -polonium crystals, Phys. Rev. B 86 (5) (2012) 054115.
- [23] K. Peterson, B. Shepler, J. Singleton, The group 12 metal chalcogenides: an accurate multireference configuration interaction and coupled cluster study, Mol. Phys. 105 (9) (2007) 1139–1155.
- [24] C.S. Nash, W.W. Crockett, An anomalous bond angle in (116) h<sub>2</sub>. theoretical evidence for supervalent hybridization, J. Phys. Chem. A 110 (14) (2006) 4619–4621.
- [25] A. Boukra, A. Zaoui, M. Ferhat, Ground state structures in the polonium based ii–vi compounds, Solid State Commun. 141 (9) (2007) 523–528.
- [26] R. Ayala, J.M. Martinez, R.R. Pappalardo, A. Munoz-Paez, E.S. Marcos, Po (iv) hydration: a quantum chemical study, J. Phys. Chem. B 112 (17) (2008) 5416–5422.
- [27] K. Rijpstra, A. Van Yperen-De Deyne, J. Neuhausen, V. Van Speybroeck, S. Cottenier, Solution enthalpy of po and te in solid lead–bismuth eutectic, J. Nucl. Mater. 450 (1–3) (2013) 287–291, <http://dx.doi.org/10.1016/j.jnucmat.2013.07.004> special Theme Issue on Spallation Materials Technology. Selected papers from the Eleventh International Workshop on Spallation Materials Technology (IWSMT-11).
- [28] A. Van Yperen-De Deyne, K. Rijpstra, M. Waroquier, V. Van Speybroeck, S. Cottenier, Binary and ternary Po-containing molecules relevant for LBE cooled reactors, JNM 458 (2014) 288–295.
- [29] P. Hohenberg, W. Kohn, Inhomogeneous electron gas, Phys. Rev. 136 (1964) B864–B871.
- [30] W. Kohn, L.J. Sham, Self-consistent equations including exchange and correlation effects, Phys. Rev. 140 (1965) A1133–A1138.
- [31] G. Kresse, J. Furthmüller, Efficient iterative schemes for ab initio total-energy calculations using a plane-wave basis set, Phys. Rev. B 54 (1996) 11169.
- [32] P.E. Blöchl, Projector augmented-wave method, Phys. Rev. B 50 (1994) 17953–17979.
- [33] G. Kresse, D. Joubert, From ultrasoft pseudopotentials to the projector augmented-wave method, Phys. Rev. B 59 (1999) 1758.
- [34] J. Perdew, K. Burke, M. Ernzerhof, Generalized gradient approximation made simple, Phys. Rev. Lett. 77 (1996) 3865–3868.
- [35] J. Hafner, Ab-initio simulations of materials using vasp: density-functional theory and beyond, J. Comput. Chem. 29 (13) (2008) 2044.

- [36] D. Hobbs, G. Kresse, J. Hafner, Fully unconstrained noncollinear magnetism within the projector augmented-wave method, *Phys. Rev. B* 62 (2000) 11556–11570, <http://dx.doi.org/10.1103/PhysRevB.62.11556>.
- [37] A. MacDonald, W. Pickett, D. Koelling, A linearised relativistic augmented-plane-wave method utilising approximate pure spin basis functions, *J. Phys. C Solid State Phys.* 13 (14) (1980) 2675.
- [38] F. Bloch, Bemerkung zur Elektronentheorie des Ferromagnetismus und der elektrischen Leitfähigkeit, *Z. Phys.* 57 (1929) 545–555.
- [39] H. Monkhorst, J. Pack, Special points for brillouin-zone integretations, *Phys. Rev. B* 13 (1976) 5188–5192.
- [40] M. Methfessel, A. Paxton, High-precision sampling for brillouin-zone integration in metals, *Phys. Rev. B* 40 (6) (1989) 3616.
- [41] A. Hermann, J. Furthmüller, H.W. Gaggeler, P. Schwerdtfeger, Spin-orbit effects in structural and electronic properties for the solid state of the group-14 elements from carbon to superheavy element 114, *Phys. Rev. B* 82 (15) (2010) 155116.
- [42] A.V. Mitin, C. van Wüllen, Two-component relativistic density-functional calculations of the dimers of the halogens from bromine through element 117 using effective core potential and all-electron methods, *J. Chem. Phys.* 124 (6) (2006) 064305.
- [43] V. Pershina, Relativistic electronic structure studies on the heaviest elements, *Radiochim. Acta Int. J. Chem. Aspects Nucl. Sci. Technol.* 99 (7–8) (2011) 459–476.
- [44] P. Błoński, J. Hafner, Geometric and magnetic properties of pt clusters supported on graphene: Relativistic density-functional calculations, *J. Chem. Phys.* 134 (15) (2011) 154705.
- [45] J.L. Da Silva, C. Stampfl, M. Scheffler, Converged properties of clean metal surfaces by all-electron first-principles calculations, *Surf. Sci.* 600 (3) (2006) 703–715.
- [46] L. Giordano, G. Pacchioni, T. Bredow, J.F. Sanz, Cu, Ag, and Au atoms adsorbed on TiO<sub>2</sub> (110): cluster and periodic calculations, *Surf. Sci.* 471 (1) (2001) 21–31.
- [47] E.W. Hansen, M. Neurock, First-principles-based monte carlo methodology applied to O/Rh(100), *Surf. Sci.* 464 (2) (2000) 91–107.
- [48] L. Vitos, A. Ruban, H.L. Skriver, J. Kollar, The surface energy of metals, *Surf. Sci.* 411 (1) (1998) 186–202.
- [49] G. Kresse, J. Hafner, First-principles study of the adsorption of atomic H on Ni (111),(100) and (110), *Surf. Sci.* 459 (3) (2000) 287–302.
- [50] S. Ohno, S. Miyahara, Y. Kurata, Experimental investigation of lead-bismuth evaporation behavior, *J. Nucl. Sci. Technol.* 42 (7) (2005) 593–599.
- [51] V. Sobolev, Thermophysical properties of lead and lead–bismuth eutectic, *J. Nucl. Mater.* 362 (2) (2007) 235–247.